JAIDS Journal of Acquired Immune Deficiency Syndromes
30:41–58 © 2002 Lippincott Williams & Wilkins, Inc., Philadelphia

Dynamics of Naive and Memory CD4$^+$ T Lymphocytes in HIV-1 Disease Progression

*†Seema H. Bajaria, ‡Glenn Webb, §Miles Cloyd, and *Denise Kirschner

*Departments of *Microbiology and Immunology and †Biomedical Engineering, The University of Michigan Medical School, Ann Arbor, Michigan; ‡Department of Mathematics, Vanderbilt University, Nashville, Tennessee; and §Department of Microbiology and Immunology, University of Texas Medical Branch, Galveston, Texas, U.S.A.*

Summary: Understanding the dynamics of naive and memory CD4$^+$ T cells in the immune response to HIV-1 infection can help elucidate typical disease progression patterns observed in HIV-1 patients. Although infection markers such as CD4$^+$ T-cell count and viral load are monitored in patient blood, the lymphatic tissues (LT) have been shown to be an important viral reservoir. Here, we introduce the first comprehensive theoretical model of disease progression based on T-cell subsets and virus circulating between the two compartments of LT and blood. We use this model to predict several trademarks observed in adult HIV-1 disease progression such as the establishment of a setpoint in the asymptomatic stage. Our model predicts that both host and viral elements play a role in determining different disease progression patterns. Viral factors include viral infectivity and production rates, whereas host factors include elements of specific immunity. We also predict the effect of highly active antiretroviral therapy and treatment cessation on cellular and viral dynamics in both blood and LT. **Key Words:** HIV-1—Homing—Naive—Memory—HAART—Mathematical model.

To date, the mechanisms that lead to the depletion of an HIV-1–infected individual's blood CD4$^+$ T cells over a typical 10-year period of progression remain unclear. Further, the pathways that drive a relatively constant viral titer during much of the disease to significantly increase during end-stage disease are also unknown. Most clinical indications of progression are based on blood data, because these data are most easily obtained. Most infection occurs in lymphatic tissues (LT), however, where 98% of CD4$^+$ T lymphocytes reside (1). Understanding the dynamics within this compartment is vital to uncovering information regarding cellular infection and viral production (2). Recent evidence indicates that lymphocyte circulation between blood and LT, which occurs as a normal process of immune surveillance in uninfected individuals, is also important when studying the effects of HIV-1 on blood lymphocytes (3–5).

Naive and memory CD4$^+$ T-lymphocyte subsets have differing roles during an immune response, which are hypothesized to be important in HIV-1 disease progression and treatment. Our goal is to elucidate their roles and describe the pathogenesis of HIV-1 infection based on host cellular and viral factors in the blood and LT. We use mathematical modeling as our experimental method. This allows synthesis of the complex dynamics occurring during the host-pathogen interaction with HIV-1 and enables us to predict the mechanisms behind different outcomes observed in patients.

In previous work, we developed a model of lymphocyte circulation between blood and LT in which HIV-1 binding to lymphocytes causes accelerated homing to the lymph nodes and increased susceptibility to homing-induced apoptosis (3). This model, which tracked productively, latently, and abortively infected cells, supported the hypothesis that homing-induced apoptosis of

Address correspondence and reprint requests to Denise Kirschner, Department of Microbiology and Immunology, 6730 Medical Science Building II, The University of Michigan Medical School, Ann Arbor, MI 48109-0620 U.S.A; e-mail: kirschne@umich.edu

Manuscript received July 24, 2001; accepted January 23, 2002.

nonproductively infected cells is a key mechanism for $CD4^+$ T-cell depletion (3). Comparison with data validated the model as a potential hypothesis for disease progression in both compartments. We did not monitor viral load directly, however. In this article, we introduce naive and memory subclasses of $CD4^+$ T cells together with virus in both the blood and LT to determine more mechanistically the dynamics of HIV-1 disease progression. By validating our model with experimental data, we can use it to predict effects of highly active antiretroviral therapy (HAART) and to interpret clinical results observed with therapy and during treatment interruption.

DYNAMICS OF A HEALTHY IMMUNE SYSTEM

Cell Phenotypes

To understand the dynamics of cells during HIV-1 infection, we first describe them in a healthy uninfected host. Newly generated naive $CD4^+$ T lymphocytes are input into the blood from the thymus. When naive cells are stimulated, those that survive their role as effector cells develop into memory cells. Combined expression of several phenotypic markers is necessary to identify a "pure" naive or memory population (1,6). Among several indicators, the CD45 protein is the most common marker for labeling a nonactivated cell as naive ($CD45RA^+$) or memory ($CD45RO^+$). For consistency between studies, we consider $CD4^+$ T cells with the $CD45RA^+$ and $CD4^+$ markers and with no prior activation or exposure to antigen to be naive, whereas memory $CD4^+$ T cells are those with the $CD45RO^+$ and $CD4^+$ markers that have previously undergone activation. We also accept that intermediates may exist based on differential expression of other proteins (7,8). Thus, when referring to data from the literature on naive and memory cells, this is the default status unless otherwise stated.

Lymphocyte Circulation

The lymph node (LN) is the area to which T cells, B cells, and antigen-presenting cells migrate to initiate and participate in the adaptive immune response to foreign pathogens (9). The adhesion molecule L-selectin (CD62L) expressed on naive $CD4^+$ T cells is essential for entry of cells into the LN. The process of lymphocytes circulating to the LNs in this fashion is referred to as homing (7). Of the more than 10^{11} immune system cells that are in constant circulation between the blood and LT, only a small proportion of memory cells (10%) travel to the LNs on a regular basis. The other 90% circulate to the spleen (50%), lung, liver, bone marrow, and other parts of the lymphoreticular system (1,10). The purpose of this trafficking is to maintain immune surveillance in all parts of the body so as to mobilize cells to sites of secondary antigen challenge (7). It is these mechanisms of homing that are altered during HIV-1 infection (see below).

Blood data can only provide a snapshot of immune and viral interaction taking place in LT. By developing a model of lymphocyte circulation between blood and LT, we can compare experimental data (from blood) while studying the dynamics occurring in LT. To this end, we first develop a virtual model of adult human lymphocyte circulation by incorporating the known circulation characteristics of naive and memory cells between the blood and LT. Our model system is depicted in Figure 1.

We develop a mathematical system to describe the interactions in Figure 1 and estimate associated param-

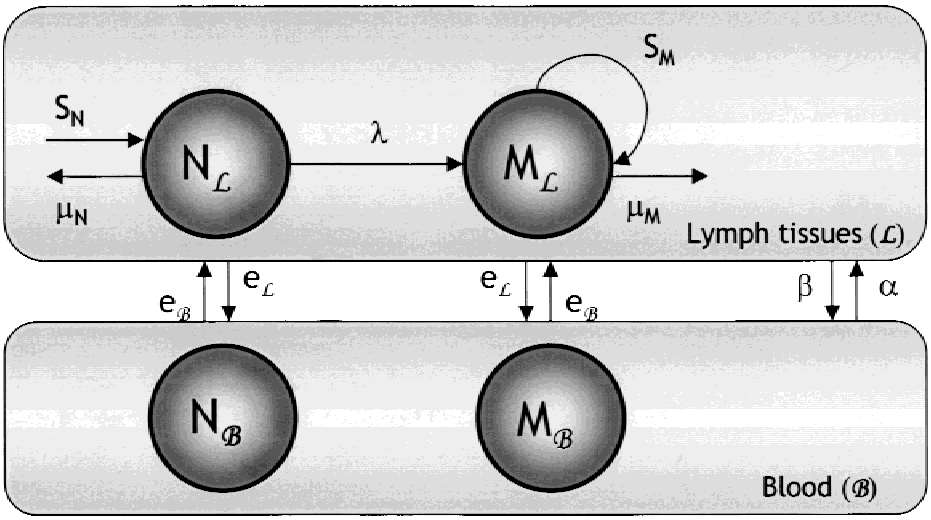

FIG. 1. Healthy model. A two-compartment model of the dynamics of $CD4^+$ naive (N) and memory (M) cells undergoing normal processes of lymphocyte circulation within blood ($\mathcal{B}$) and lymphatic tissues ($\mathcal{L}$), where e = circulation between blood and lymph tissues, λ = differentiation, S = proliferation, and μ = death. The α and β parameters are scaling terms for compartmental exchange.

eters from the literature (Table 1 in Appendix). We then simulate the model by solving the differential equation system using appropriate numeric methods. The results of the computational experiments are shown in Figure 2 for a representative 10-year period.

Our simulation is comparable to experimental data on age-related decline of $CD4^+$ naive T cells (11–13). The proliferation of memory $CD4^+$ T cells allows the total $CD4^+$ T-cell count to remain at a relative steady state over long periods, despite the continual decline in the number of new naive cells supplied by the thymus as a result of involution. The total number of $CD4^+$ T cells in blood remains at approximately 1000 cells/mm^3 with some evidence for a gradual depletion over time (14,15), also shown in Figure 2. This supports the theory of Haase (16) and others who assert that homeostatic mechanisms maintain a quasi–steady-state population in which there is a balance of the growth of one compartment with death in the other. Our model system thus reflects the homeostasis that is observed in total $CD4^+$ T-cell counts in blood and LT in an average healthy adult (17). We explored variations in parameters that do not have a direct estimate from the literature (see estimates in Table 1 in Appendix). Results indicate that if either the direct differentiation from naive to memory cells or the proliferation of memory cells is increased (Equation 6 in Appendix), there is an overall higher population of memory cells, but homeostasis is still maintained. If the parameters for memory cell proliferation are decreased by orders of magnitude, homeostasis is not achieved. Therefore, our model predicts that the processes of memory cell production are crucial to maintaining T-cell levels in steady state.

HIV-1 INFECTION IN THE HUMAN HOST

Disease Progression

Adult infection with HIV-1 results in three relatively common clinical periods of acute, asymptomatic, and end-stage disease, despite the patient-specific interaction of the pathogen with the human immune system. A viral setpoint is established in the acute stage and is thought to determine the speed of progression to AIDS (18,19). End-stage disease results in three common disease scenarios. Long-term nonprogressors (LTNPs) are a small percentage (5%–10%) of the infected population who evade the typical progression to AIDS without the help of antiretroviral therapy for as long as 20 years (18,20, 21). In contrast, individuals whose $CD4^+$ T-cell levels decrease below 200 cells/μL after the 8- to 10-year asymptomatic period while virus levels in end-stage disease increase exponentially are characterized as typical progressors (22). Finally, some individuals develop AIDS within 3 to 5 years after initial infection and are known as rapid progressors. In this case, an unusually early decline in $CD4^+$ T-cell count may be caused by infection with a particularly cytopathic strain or may occur in individuals who are more susceptible to AIDS based on factors such as immune status at the time of infection, age, and genetic profile. Our model predicts that a disruption in normal homeostasis of naive and memory cells is a crucial factor in determining an individual's disease progression.

HIV-1 Virus Effect on Lymphocyte Circulation and Cellular Infection

Although conflicting hypotheses exist as to which $CD4^+$ T-cell subset is preferentially infected by HIV-1, several studies support selective naive cell depletion early in disease progression (23,24). One reason for this may include enhanced homing-induced apoptosis of naive cells (5,25). There is also evidence for greater depletion of thymus-derived naive ($CD45RA^+$ $CD62L^+$) $CD4^+$ T cells early in infection beyond involution (26–29).

A major change induced by HIV-1 binding is an alteration in lymphocyte circulation. HIV-1 can signal $CD45RO^+$ $CD4^+$ T cells to undergo homing to lymph nodes, a great deviation from their normal travel

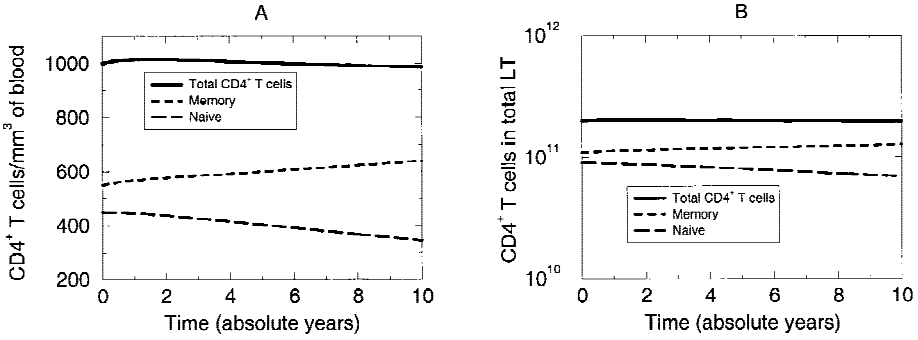

FIG. 2. Healthy model results. Temporal dynamics of naive (*long dashes*), memory (*short dashes*), and total (*solid line*) lymphocytes during a representative 10-year period in a healthy uninfected host. **(A)** Populations in the blood (linear scale). **(B)** Populations in the lymphatic tissues (log scale). The parameters and initial values used in the simulations are given in Table 1 in the Appendix.

throughout the lymphoreticular system (25). Steady-state levels of virus in the LT during the asymptomatic period of infection disguise effects to lymphocyte homing and circulation mechanisms. Throughout the course of the disease, naive cells continue to home but at an accelerated rate, whereas memory cells are recruited from their peripheral circulation to participate in LT homing (25). Memory T cells that circulate through the peripheral tissues are spared; however, memory and naive cells circulating through the LT are constant targets for viral infection or virus-induced signaling as a result of contact with virions or virus-producing cells (30). Given this HIV-1–induced memory cell circulation pattern, both memory (activated) and naive cells that come in contact with HIV-1 are equally susceptible to apoptosis after signaling through homing receptors (L-selectin or $CD62L^+$) occurs (25). Signaling of $CD62L^+$ and other homing receptors can induce apoptosis of HIV-1–signaled T lymphocytes in as much as 30% to 50% of abortively infected (HIV-1–signaled) resting or activated cells (5,25,31).

Activation-induced cell death has also been implicated as a major cause of $CD4^+$ T-cell depletion. Several sources link activation-induced cell death with homing-induced apoptosis as described previously by showing that activation is a direct cause of apoptosis of the host cell or that activation is associated with apoptosis in virus-negative cells (32,33). When infected cells or free virions bind with neighboring uninfected cells, the uninfected cells become signaled, although they do not produce viral RNA (the "bystander effect") (34,35).

We clarify for our purposes the different cell phenotypes in our model. Productively infected cells [approximately 1 in 100,000 T cells (36)] are activated cells; thus, viral DNA can enter the nucleus. These cells are able to produce viral progeny, and survive no more than 2 days (37). Provirus can survive for months or years, resulting in a latently infected cell. If HIV-1 DNA is unable to integrate into the nucleus and remains in the cytoplasm of resting (naive or memory) host cells, it is unstable and decays after a few days (25,31,36,38). These cells are referred to as abortively infected cells. Abortive infection can induce upregulation of L-selectin, causing most of these cells to home. They return to the naive class after viral DNA degrades and may participate in further homing or infection activities (25,31,36). Because 95% to 99% of T cells are resting at any given time, most infections are abortive (39,40).

The model developed here elucidates possible mechanisms describing differences in disease progression based on the differential interaction of the HIV-1 virus with the naive and memory subclasses of $CD4^+$ T cells together with effects to lymphocyte circulation. Our goal is to build on our healthy model by including HIV-1 infection. We maintain varying circulation characteristics of memory and naive cells as in the baseline model and include their individual susceptibilities to infection. Infection directly produces abortive and productively infected classes of cells that are assumed to be present predominantly in the LT compartments owing to the assumption that infected cells in the blood (containing only 2% of all T cells) constitute a relatively small contribution to overall infection and that most HIV-1 replication occurs in the LT (39–42). Latently infected cells are derived only from productively infected cells that have deactivated (31,43). A cell that has become abortively infected is increased in its homing capability by upregulation of L-selectin. Therefore, it is believed that most of these cells either undergo apoptosis or revert to the naive class if they have not been signaled through their antigen receptors. Any cell that becomes productively infected (whether memory or naive) must have been activated and thus is counted as a memory cell until its death. Memory cells and productively infected cells have a higher death rate than naive cells (as a result of activation-induced cell death) (32). Figure 3 depicts the dynamics of naive, memory, and infected cells as well as virus within the two compartments of blood and LT.

We develop a mathematical system to describe the terms in Figure 3 and estimate associated parameters from the literature (summarized in Appendix; see Table 2 in Appendix). We again simulate the model by solving the differential equation system using appropriate numeric methods. We discuss below the results of the computational experiments in two scenarios: long-term nonprogressive infection and typical progression.

Long-Term Nonprogressors

Our purpose in developing a virtual human LTNP model is to predict mechanisms responsible for the dynamics of lymphocyte circulation patterns of naive and memory cells in an HIV-1–infected patient during the primary, asymptomatic, and end stages of infection. Similar to others (44), we also consider the dynamics of memory and naive $CD4^+$ T cells to play significant roles in the comprehensive picture of infection. We examine the behavior of these two cell populations in the blood and LT over the course of disease, monitor viral load, and compare model simulations with clinical data. Once this is achieved, we can use the model to ask questions about underlying mechanisms of LTNP progression. Figure 4 portrays our model simulation of LTNP progression. Panels A, B, and C encompass cellular and viral dynamics in the acute stage. Our simulations cor-

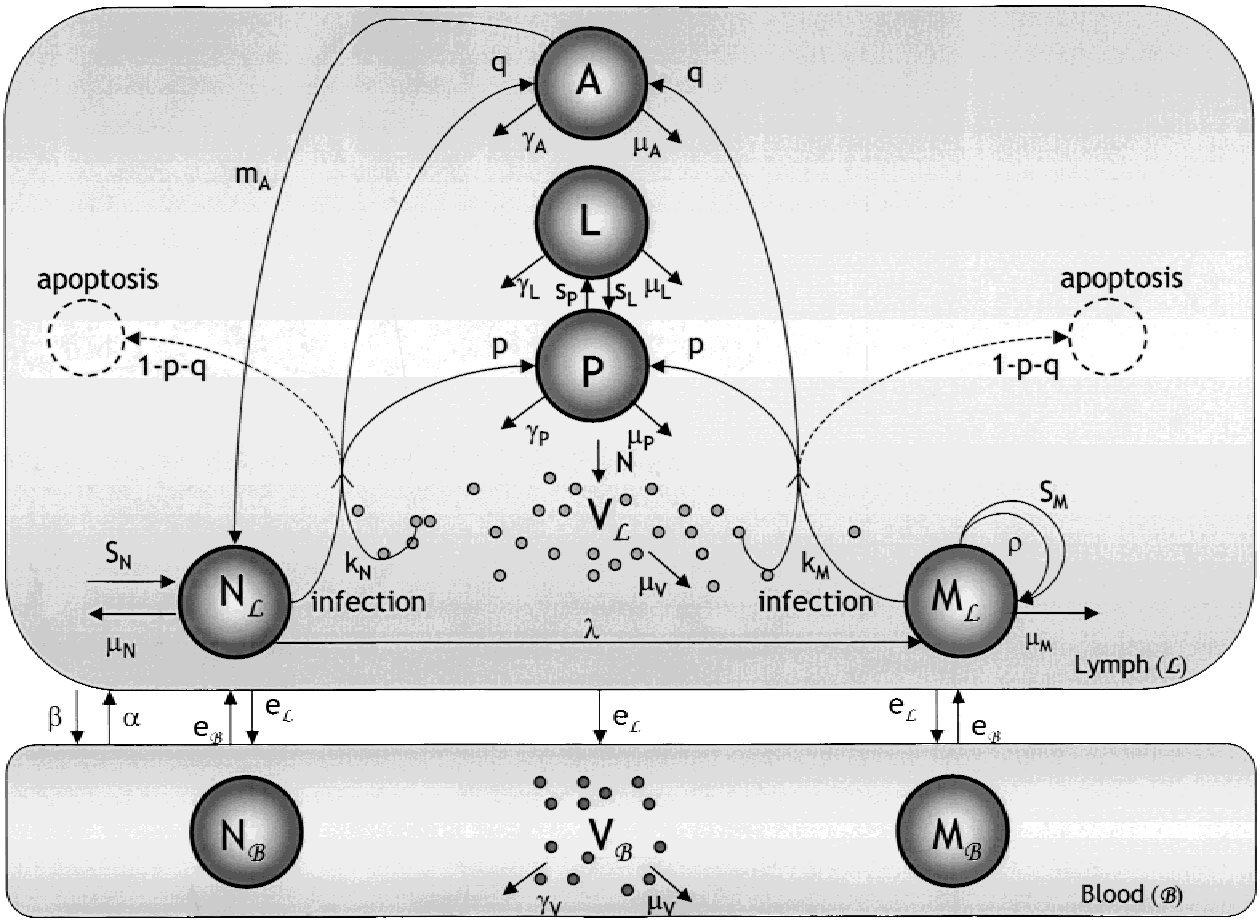

FIG. 3. HIV-1 model. A two-compartment model of the dynamics of CD4+ memory (M) and naive (N) cells during HIV-1 (V) infection within blood ($\mathcal{B}$) and lymphatic tissues (LT) ($\mathcal{L}$), where A, L, and P = abortively, latently, productively infected cells, respectively; e = circulation between blood and LT; λ = differentiation; S = source/proliferation; ρ = clonal expansion; μ = death; γ = immune clearance; p, q = proportion of infected cells that become productively and abortively infected, respectively; s = activation/deactivation; k = infection, and m = reversion to uninfected status.

relate with findings that there is a dramatic drop in CD4+ T-cell counts 3 to 6 weeks after infection (48). Panel *D* depicts long-term dynamics in the blood from our model compared with representative data over the simulated 10-year disease course. Results were compared with those of six patients in a study of LTNP who showed a similar steady level of CD4+ T cells over the course of 10 years (45). Table 3 presents a comparison of the model simulations in LT with proportional data for each class of infected cells, uninfected cells, and free virus (measured as HIV-1 RNA). By validating the results of our model against clinical data, we then use this model to test further theories of the lymphocyte-viral interaction.

Key Parameter Dynamics

Because reaction rates likely vary among individuals and studies, parameter values used in the model are not exact. It is important to explore effects to the model through uncertainty and sensitivity analyses based on parameter variation (49). Such experiments can elucidate model elements that may most significantly contribute to the rapidity at which an individual progresses to AIDS as well as to the overall pattern of lymphocyte depletion and virus growth.

Our model predicts that several key parameters must lie within a specific range to exhibit the standard behavior of a typical HIV-1 LTNP. We explore five key parameters that are capable of dramatically changing the typical course of disease. The primary effects of their variation resulted in changes in onset of acute-stage disease and rapidity of progression to AIDS. These five parameters encompass both host factors and viral factors, indicating that all play significant roles in disease progression. Here, virulence factors of the virus include its

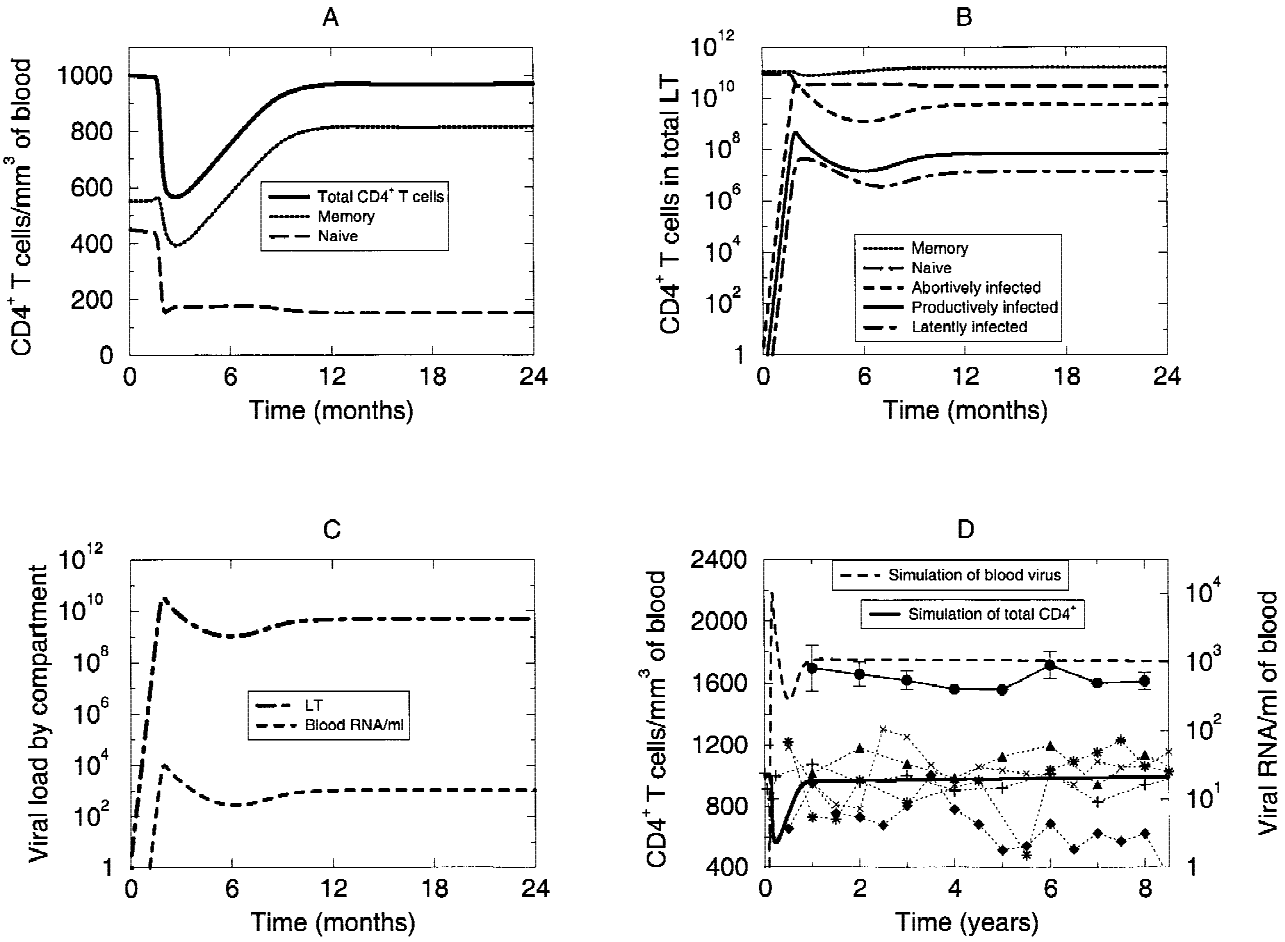

FIG. 4. Long-term nonprogressor (LTNP) model results. **(A–C)** Acute and asymptomatic stages for cell classes in blood, cells in lymphatic tissues (LT), and virus in both LT and blood, respectively. (**D**) Comparison of our model solution for longer than 8 years of infection with data from Pantaleo et al. (45), Greenough et al. (46), and Fauci et al. (47) for $CD4^+$ counts (♦, +, ×, ▲, ✳) and from Pantaleo et al. (45) for viral load (●) in the typical LTNP. The parameters and initial values are given in Table 2 in the Appendix (see Table 3 for further comparison with data).

ability to infect cells as well as to produce progeny, where an increase in either mechanism indicates an enhanced ability for sustained immune evasion. Host factors that play a role in HIV-1 infection likely involve production of antigen-specific $CD4^+$ and $CD8^+$ T cells against virus and virally infected cells as well as increased proliferation of uninfected cells. We elaborate these results as follows.

Viral Factors

Infection rate of naive cells by virus (k_N). A low ability to infect naive cells results in a higher $CD4^+$ T-cell steady state and a lower viral set point. Extremely low values of this parameter can result in clearance of virus and no effect to homeostasis of uninfected cells. A

TABLE 3. *Long-term nonprogressor model simulation values compared with experimental data in lymphatic tissues*

Cells by type in lymphatic tissues	Model value after 10 years	Experimental value(s)	References
Latently infected cells	1.4×10^7 cells	1.0×10^5–1.2×10^7 cells	39, 67
Productively infected cells	7.0×10^7 cells	1.4×10^6–5.0×10^8 cells	16, 25, 36
Abortively infected cells	6.0×10^9 cells	10^9 cells	40
Viral production	2.0×10^{10} virions/cell	10^{10} virions/cell	99
Viral load	5.0×10^9 virions	10^8–10^{11} virions	40

large increase leads to a much higher viral setpoint with immediate depletion of naive cells.

Infection rate of memory cells by virus (k_M). A low ability to infect memory cells results in a lower viral setpoint and a higher $CD4^+$ T-cell steady state. Extremely low values of k_M produce a pronounced viral decline and absence of a viral setpoint rather than viral clearance, however. Large values of k_M also lead to higher setpoints and low levels of $CD4^+$ memory T cells but not depletion.

Average number of virions produced by productively infected cells (N). Experimental data indicate that the average number of virions produced from a productively infected cell is between 100 and 1000 virions per day per cell (25,50,51). Our model shows that values on extreme ends of this range maintained throughout infection can dramatically alter disease course; low values result in viral clearance, whereas high values result in an elevated setpoint and a low total $CD4^+$ T-cell steady state.

Host Factors

Clearance rate of productively infected cells from LT (γ_P). A previous model examined the effects of an immune response to high viral levels produced during acute infection, affecting the rate of viral decrease to asymptomatic levels (52). Similarly, we consider the effects of a variable immune response in both blood and LT. Varying the strength of the immune response over six orders of magnitude reveals that the immune response against productively infected cells is of key importance. If the immune response is extremely efficient from the first day of infection (γ_P on the order of 10^{-11}per day per cell), the individual may clear virus. Thus, our results imply that the strength of the immune response to infection plays a significant role in an individual's eventual disease progression.

Clearance rate of free virus from blood (γ_V). Another example of the fine balance between host and viral factors can be shown by variation of immune clearance in the blood (γ_V). By varying this parameter over several orders of magnitude, our model captures varied ability of the immune response to combat infection. This experiment produces different viral set point levels (Fig. 5) (19).

Note that variation in any of the 5 parameters discussed can produce the different viral setpoints.

Typical Progressors

Our LTNP virtual human model depicts steady-state viral levels (after the acute stage) throughout the simulated 10-year course of infection. If HIV-1 maintained constant virulence and the host immune response persisted (as in primary infection), the individual would exhibit the behavior of the LTNP model indefinitely. As we know through several decades of HIV-1 history, how-

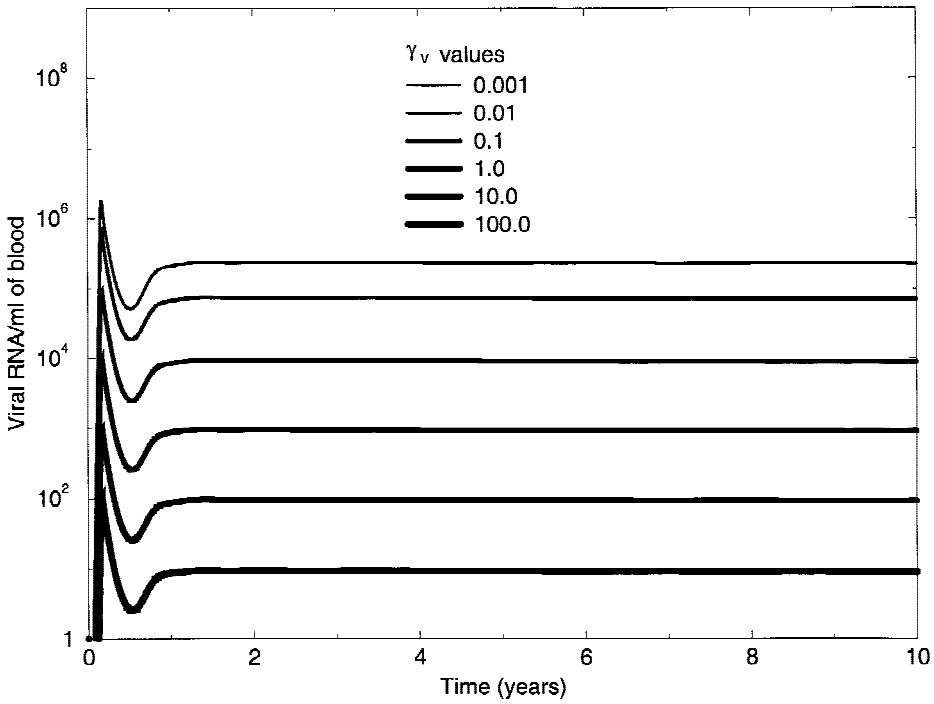

FIG. 5. Effect of varying the strength of the immune response (γ_V) in the blood on the viral set point. The increasing strength of the immune response is indicated by increasing line thickness (from top to bottom), with exact values for the parameter γ_V varying from 0.001 to 100.0 as shown in the legend. Other parameters and initial values are identical to those given in Table 2 in the Appendix for the long-term nonprogressor model.

ever, this is generally not the case. Clinical data indicate that for most individuals not receiving therapy, $CD4^+$ T-cell levels in blood are constantly decreasing, with a dramatic increase in virus in the final stages of disease. To realize the viral increase observed in HIV-1 typical progressor patients during end-stage disease, there must likely be elements of the host-pathogen dynamic that change over the long-term course of infection. It is believed that HIV-1 uses one or more mechanisms to evolve and vary antigenically during infection. We consider these strategies as viral factors. Alternatively, the host may eventually lose mechanisms (host factors) that effectively contain viral growth. Likely candidates for host-disease elements that may evolve over time to produce AIDS in late disease are those that resulted in significant variation in simulations when tested over a large range in the baseline model (see previous section).

HOST AND VIRAL INFLUENCES

Virus Factors

HIV-1 is thought to become more virulent through various mechanisms during the course of disease. After sexual transmission, HIV-1 primarily uses the CCR5 coreceptor expressed on $CD4^+$ T cells (53). In many cases, the virus may evolve to use both CCR5 and CXCR4 or CXCR4 exclusively (16,23,53–55). Because CXCR4 is thought to be present on most T cells (24), we represent the increasing coreceptor repertoire by allowing the infection rates (k_N and k_M) to increase linearly throughout disease progression in both cell subsets (variations in this linear increase were also tested). There is also the likelihood of greater replication ability over the course of disease. This evolution could result from an increase in the number of virions (N) produced by productively infected cells during the course of infection (56,57). We model the viral production number as also increasing linearly from our initial value of 500 virions per day per cell to 1000 virions per day per cell.

It is likely that in the rare rapid progressor scenario, patients begin with rates of infection or viral production so high that AIDS appears within 3 to 5 years. Increasing the initial infection rates or the viral production rate or accelerating their respective time-dependent increases (as in the typical progressor model) by much greater amounts than described previously results in behavior typical of rapid progressors (data not shown).

Other virus factors that may maintain an infected individual in the asymptomatic stage could be specific to viral strain. For example, deletions or mutations in the *nef* gene of the HIV-1 viral envelope have been shown to correlate with slower progression to AIDS (58).

Host Factors

In addition to an alteration in the numbers of $CD4^+$ T cells, $CD8^+$ T cells are also affected by HIV-1 infection. The loss of $CD4^+$ cells is compensated for by a gain in the number of $CD8^+$ cells (total T-cell homeostasis) (17). Although naive and memory $CD4^+$ T-cell subsets decline, $CD8^+$ naive cell numbers increase slightly and $CD8^+$ memory cell numbers increase dramatically to compensate and maintain T-cell homeostasis (17). The normal ratio for CD4 to CD8 is approximately 2:1, and reverses early in HIV^+ patients to approximately 1:2 in the blood and later in the LT (17,59,60). Our model presently includes only $CD4^+$ lymphocytes, although recent evidence suggests that $CD8^+$ T cells may also be directly infected by HIV-1 (61,62). We indirectly account for their role in eliminating virally infected cells in the immune clearance terms (Equations 11–13 and 15 in Appendix). Activated $CD8^+$ T-cells, or cytotoxic T-lymphocytes (CTLs), are thought to mainly target infected cells; however, because we do not include the small proportion of infected cells in the blood, we indirectly model blood CTL activity. This captures greater clearance of infected cells from the body when the number of uninfected immune system cells is high and a decreased ability to clear virus when $CD4^+$ T-cell levels fall (63). The function of this subset of cells is being directly modeled in ongoing work.

Memory $CD4^+$ T-cell proliferation is impaired in the presence of HIV-1 (63). By late-stage disease, $CD4^+$ T-cells encompass less than 10% of the total T-cell subsets, with $CD8^+$ T cells, particularly memory $CD8^+$ T cells, comprising the remainder (63). This is in contrast to an uninfected individual, whose $CD4^+$ counts remain at approximately 66% of the total T-cell pool (63). Thus, in the progressor scenario, we model a gradual decline in the ability of $CD4^+$ memory T cells to proliferate or clonally expand by considering a time-dependent source of memory cells.

A simulation of virtual human infection is given using the previously discussed time-dependent parameters (Fig. 6). Combinations of these factors result in a model outcome similar to that observed in the classic HIV-1 patient who progresses to AIDS (the stage at which the infected individual has less than 200 $CD4^+$ cells/mm^3 of blood) (65) in approximately 8 to 10 years.

The LTNP and typical progressor models are distinct in several dynamic aspects; however, viral load and $CD4^+$ T-cell levels are the most obvious (see Fig. 4 and 6). Recall our indirect modeling of immune activity

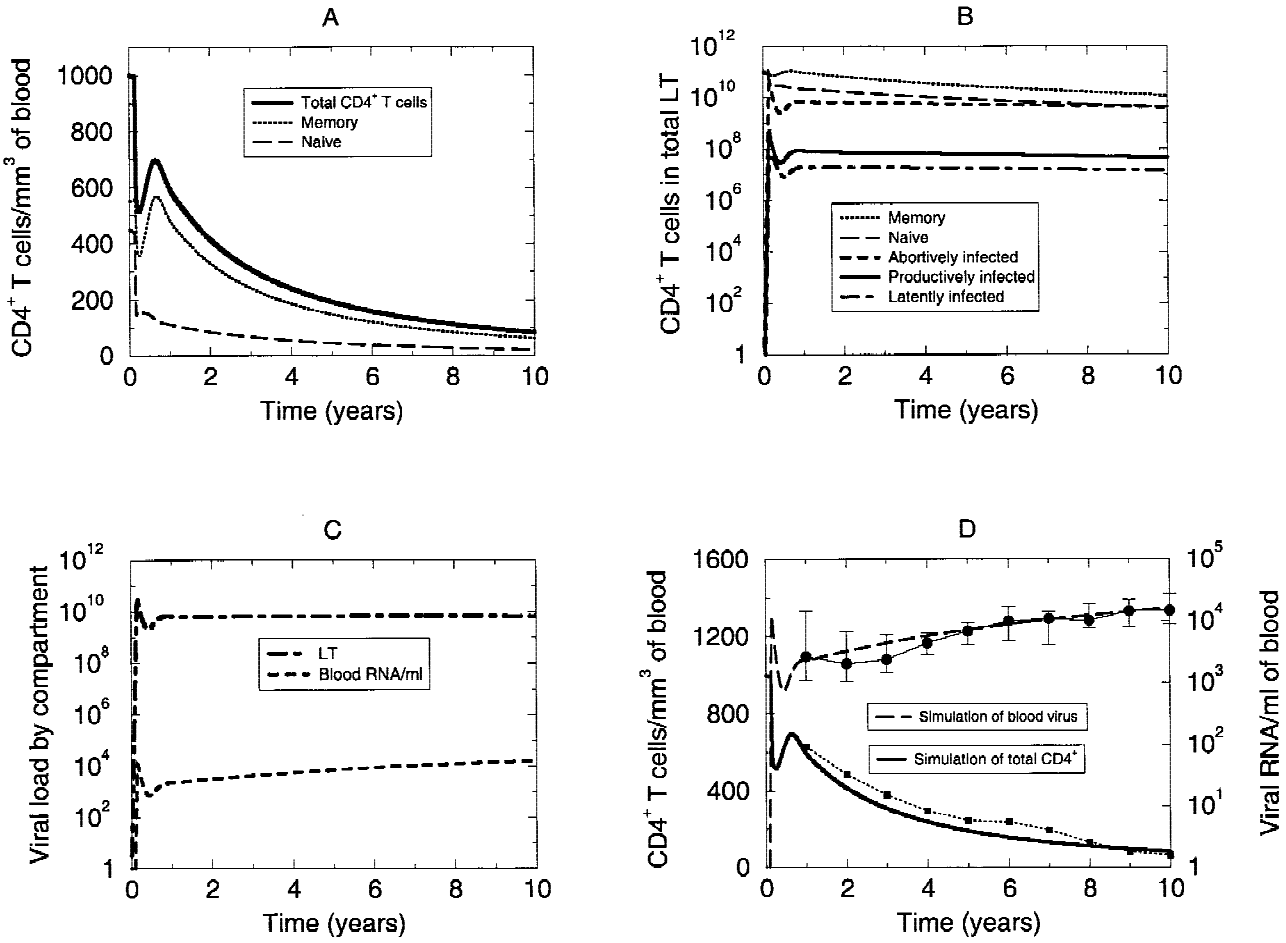

FIG. 6. Typical progressor model results. Model simulations of the typical progressor for both blood and lymphatic tissue (LT) compartments. Simulation shows average time series of $CD4^+$ T cells and virus during HIV-1 infection. Figures are for long-term disease progression, where the AIDS stage occurs within 10 years. Equation 6 in the Appendix shows S_M (memory proliferation) as constant; we modify this equation by allowing S_M to be dependent on time. This allows for a linear decrease in the proliferation capability of memory cells, representing a gradually decreasing ability to maintain homeostasis of the total $CD4^+$ T-cell count. Total $CD4^+$ T-cell population as well as subsets of memory and naive cells (**A**), the two subsets in LT as well as the three classes of infected cells (**B**), virus (**C**), and comparison with experimental data (●) from the study by Sabin et al. (64) for blood virus and from the study by Greenough et al. (46) for blood $CD4^+$ T cells (■) (**D**). The time-dependent parameters are k_N, k_M, N, S_M, and S_N as described in the Appendix. The other parameters are the same as in Tables 1 and 2 in the Appendix for the long-term nonprogressor model.

through the immune clearance terms. A high level of immune activity is observed in LTNP patients, whereas declining immune activity is associated with typical progression (66). The distinctions in immunity between a healthy individual, an LTNP, and a typical progressor are shown in Figure 7. The ability of $CD4^+$ memory T cells to maintain homeostasis as well as to clear productively infected cells decreases significantly in the progressor compared with the sustained immune activity observed in the LTNP.

HAART THERAPY

We now use our model, which is representative of several hallmarks of HIV-1 disease progression, to describe the influence of treatment on an infected individual. HAART acts by either reducing viral production or blocking de novo infection or spread and typically results in an increase in $CD4^+$ T-cell counts during the administration period. It is believed that therapy-induced suppression of viral replication reduces the number of cells that home to lymph nodes and undergo homing-induced apoptosis, thus resulting in the reappearance of blood lymphocytes (25). Additionally, some data indicate that treatment can augment thymic output (27,28). The output of new naive cells from the thymus has been hypothesized not only to recover but even to increase, countering the accelerated depletion during HIV-1 infection (27).

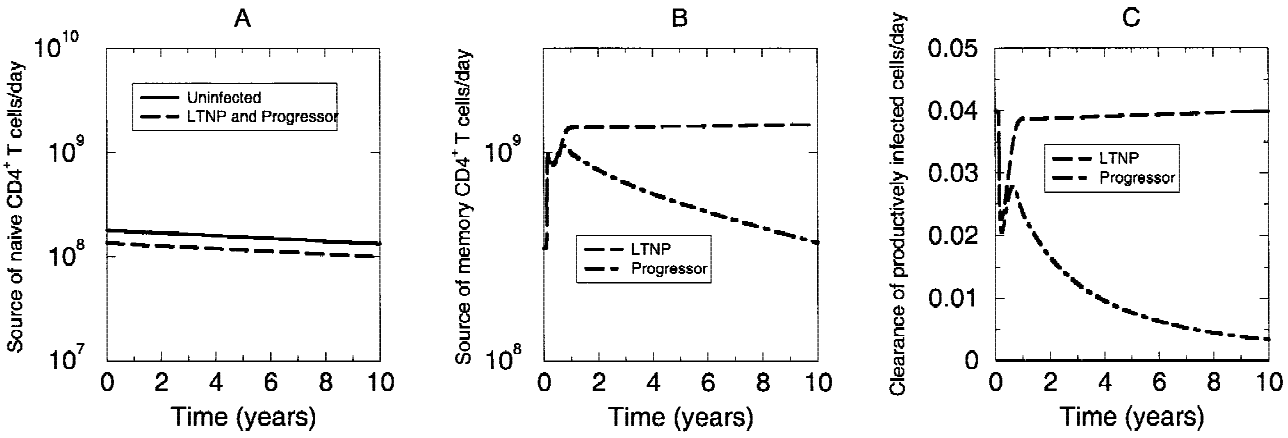

FIG. 7. Model simulations for immune activity in three scenarios: uninfected, long-term nonprogressor (LTNP), and typical progression. Depiction of the decreasing source of new naive cells from the thymus ($S_N(t)$) **(A)**; production of memory cells as a result of homeostatic mechanisms, differentiation, and clonal expansion ($S_M(t) + \lambda + \rho$) (**B**); and immune clearance of productively infected cells in the lymphatic tissues ($\gamma_P(N_{\mathcal{L}} + M_{\mathcal{L}})$) **(C)**. As seen in **B**, HIV-1–specific memory cells proliferate greatly in acute-stage disease for both LTNP and typical progressors; however, only the LTNP is able to maintain this antigen-specific expansion. Additionally, in **C**, immune activity is immediately impaired in acute-stage disease (in both LTNP and typical progressors) concomitant with the sudden decline in uninfected cell populations, but only the LTNP is able to recover the ability to clear uninfected cells. The time-dependent parameters for the progressor are k_N, k_M, N, S_N, and S_M. All other parameters for the uninfected case and LTNP are the same as in Tables 1 and 2 in the Appendix.

Clinical Response to HAART Treatment

Several clinical studies have been performed describing qualitatively and quantitatively the effects of HAART on the immune system. Most commonly, there is a biphasic or multiphasic decline in viral load (30). Virus in the blood decreases quickly for several weeks, followed by an indefinitely prolonged decline (67). Suppression of viral replication occurs such that virus levels fall to undetectable levels (defined by 20 to 500 copies/mL of blood, depending on the assay) (39, 67,68).

There are distinct dynamics of memory and naive cells during treatment. An earlier rapid rise in the memory cell class occurs at the initiation of treatment, whereas naive cells return later, with a more sustained response (1,6,16,30,69–72). Several studies indicate a biphasic repopulation of $CD4^+$ T cells: an initial increase in memory cells over the first few months of treatment, followed by a less dramatic rise lasting up to 1 year (71,73,74). One study proposed that the early return of memory cells is an interruption in HIV-1–induced circulation and virus production, whereas the slower second phase represents immune generation (69).

After cessation of drug therapy, the persistence of resting $CD4^+$ T cells carrying replication-competent HIV-1 suggests that latently infected cells are likely to be a major viral reservoir even if active virus replication is suppressed by HAART for as long as 2 years (16,54,75). The long period during which virus decays at a much slower rate can be attributed to a low level of viral transcription as well as the long half-life of latently infected cells (up to 44 months) (76,77). This effect is seen as HIV-1 rebounds promptly after cessation of drug therapy in most patients (75,78,79).

Incorporating Treatment in the Infected Model

In an actual clinical setting, there is debate as to whether HAART actually reduces viral infectivity and production to zero, despite undetectable levels of plasma virus and productively infected cells (80–82). Although many models assume that infection is completely eliminated at the onset of therapy, evidence suggests there is residual viral replication occurring below the detection limit (83). The biphasic decline also indicates that there is more than one reservoir producing infectious particles with varying lifespans even during the treatment window (67). To include HAART in our model of HIV-1 disease progression, we alter the system Equations 9, 10, and 12 through 14 (see Appendix) by reducing viral infectivity and production by 90% on the day treatment begins. The increase in thymic output during HAART is modeled by a slight increase in thymic output (1% per year; see Appendix) (28).

Our model shows the effect of administering HAART over a 108-week duration beginning 9 years after the initial infection (Fig. 8). The model predicts that there is a rapid decrease in all types of infected cells after the onset of therapy. Another relevant model outcome is the preferential elimination of infected classes. The produc-

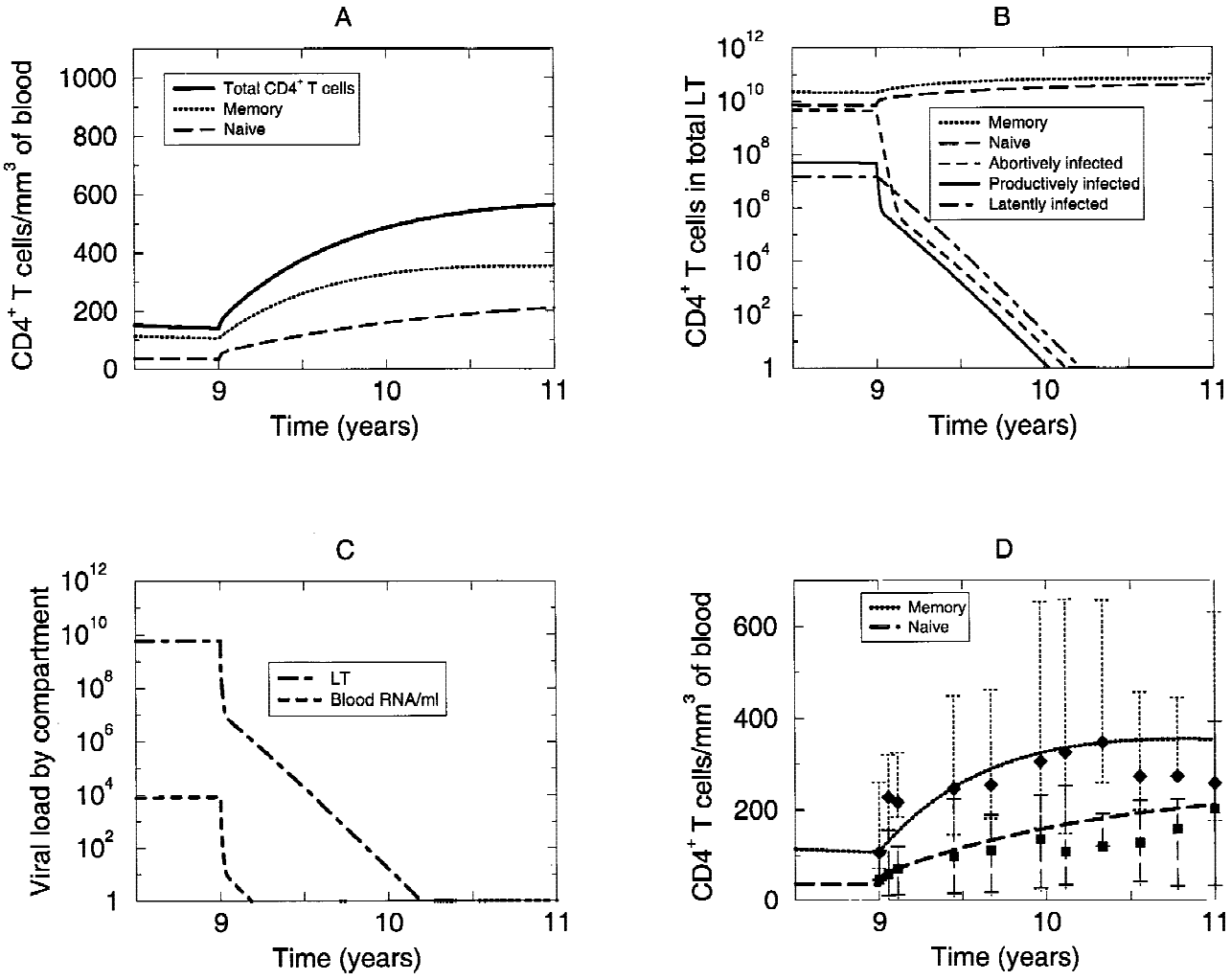

FIG. 8. Effect of highly active antiretroviral therapy (HAART) on CD4+ T cells and virus in the blood and lymphatic tissues (LT). In the model simulation, therapy was administered at 9 years and subsequently removed at 11 years. The recovery of memory and naive cells in the blood as well as their total **(A)**, infected cell classes in the LT **(B)**, virus in the LT and blood **(C)**, and comparison of CD4+ T-cell recovery with representative data from the report by Notermans et al. (85) for memory (♦) and naive (■) classes (**D**).

tively infected cells decline first as a result of their relatively short half-life (37). Abortively infected cells are the next to die out, whereas the latent reservoir declines the slowest. The characteristic biphasic decline in viral load is also observed. The sharp reduction of virus in both blood and LT within the first 4 to 12 weeks of treatment can be attributed to the relatively short half-lives of productively infected cells and free virus (78). Repopulation of the naive class is dependent on an individual's capacity for regeneration (72). We vary the rate of increase in thymic output during treatment and observe a similar result (data not shown). Cells also return to the blood compartment as a result of cessation of HIV-1–induced homing and homing-induced apoptosis; thus, an increase in the number of memory cells occurs almost immediately at the onset of therapy (31). Our simulation also predicts that the latent reservoir in resting memory CD4+ T cells fails to be eradicated over a long period (approximately 4 years; data not shown). The persistence of latently infected cells, even in undetectable amounts, causes the re-emergence of virus to more than 50 copies/mL (RNA) within weeks after discontinuing HAART (75,84).

Panel D of Figure 8 shows the model simulation compared with data for a 2-year study in which naive and memory cells were at similar levels at the onset of the triple therapy and all patients were previously naïve to treatment.

Optimal Treatment Strategies

Administration of HAART is dependent on the individual, and need is assessed on a case-by-case basis. The

ideal treatment schedule takes account of the host's ability to respond to therapy as well as the level of viral suppression. Scheduled treatment interruptions that allow the patient a temporary break from continuous treatment regimens are becoming more common and successful as suggested by mathematical modeling (86). The effectiveness of such strategies is largely based on the individual's recovery after cessation of therapy, however. Individuals with impaired immune responses, even after 2 years of therapy, may return within weeks to viral levels as high as that present at the onset of HAART. Others may be able to suppress viral replication successfully enough to experience a delay in re-emergence of virus between treatments (87). In all of our HAART simulations, treatment is administered between years 9 and 11, and stopped at year 11. Panels A and B of Figure 9 show the effects of suppressing viral production and infection during treatment between 0% and 40%, with 90% as a comparison (from Figure 8). It can be seen that when viral infectivity and production are not effectively suppressed during HAART, the viral load remains above the detection limit or even rebounds within the 2-year treatment window. Upon cessation of therapy at year 11, the level to which $CD4^+$ T-cell numbers decline and virus rebounds is dependent upon an individual's responsiveness to therapy. In Panels C and D we show the effect of varying viral rebound to between 50% and 90% of pretreatment levels. Patients whose virus returns only after a significant delay would be ideal candidates for treatment interruptions, as temporary cessation of therapy would not cause immediate viral rebound.

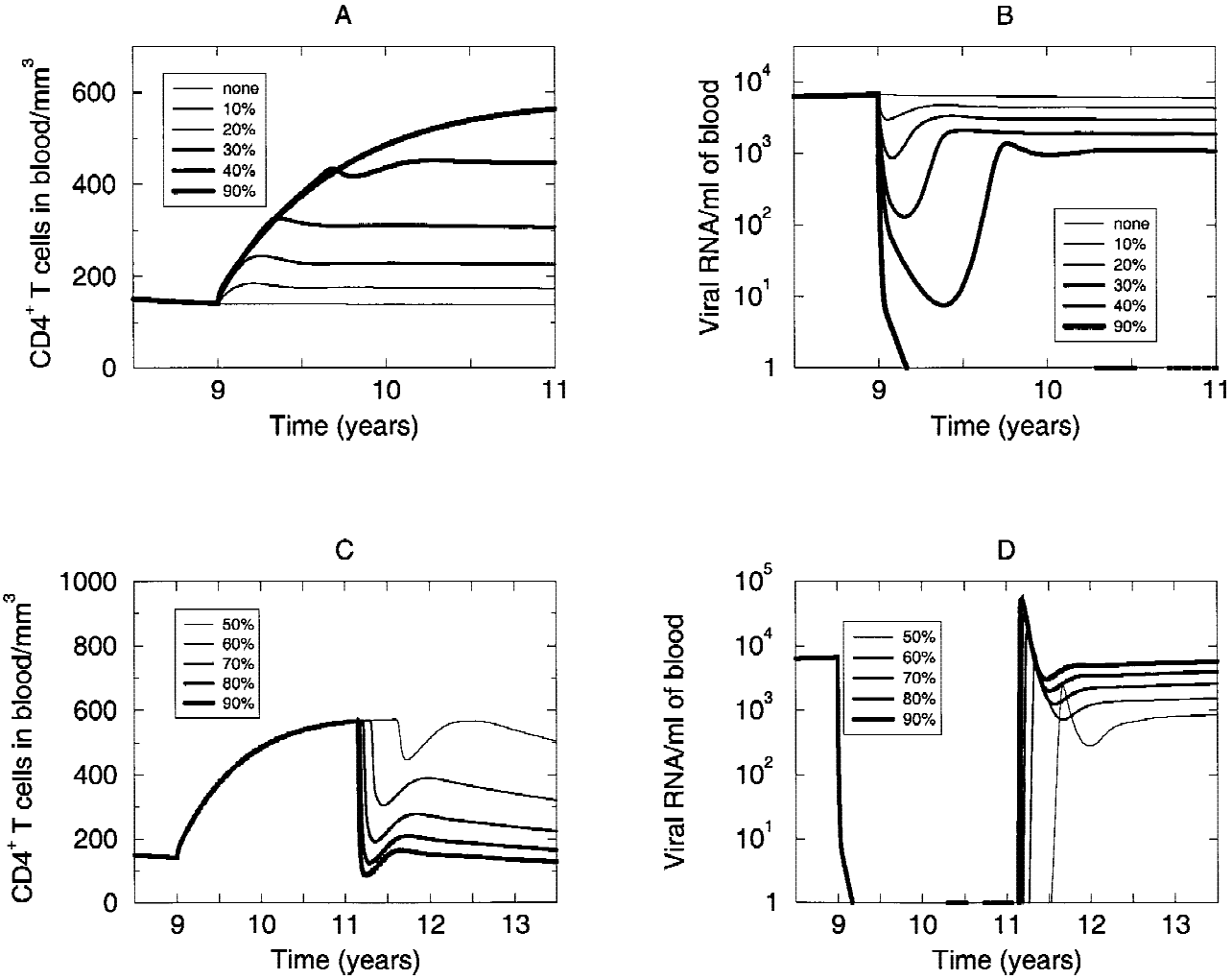

FIG. 9. Effect of varying treatment efficacy during and after a 2-year period on HAART. **(A and B)** Effect of the total $CD4^+$ T cells and virus in blood from variations in viral suppression during treatment. Percentages shown are differing levels of drug efficacy. **(C and D)** Dynamics of T-cell decline and viral rebound after cessation of therapy based on viral rebound immediately after treatment cessation (to between 50 and 90% of pretreatment levels). All other parameters are the same as for Figure 8.

Our model simulations with HAART support the experimental findings that there exists a large variation in the return of $CD4^+$ T cells after the onset of therapy. Our model predicts that both host and viral factors play a significant role in recovery and maintenance of treatment effects.

DISCUSSION

There is a significant amount of clinical and experimental data describing HIV-1 disease progression in adult humans. The mechanisms explaining the dynamics of the host-viral interaction remain unclear, however. We believe that including virus and infected cells in our model as well as the nonlinear interaction of cells with virus provides a more definitive picture of $CD4^+$ T cells and virus in the in vivo context of blood and LT.

In this work, we first develop a mathematical model to capture the dynamics of naive and memory $CD4^+$ T cells as they undergo normal growth, death, and circulation between the blood and LT in the absence of HIV-1 infection. We then introduce HIV-1 in the model to study how the known and hypothesized interactions of virus and $CD4^+$ T cells lead to different disease outcomes as seen in clinical settings. Our simulations yield the characteristic depletions of $CD4^+$ T cells in the blood together with a relatively constant number in LT. In our model, subtle mechanisms of circulation, alteration, and enhanced apoptosis of naive and memory (activated) $CD4^+$ T cells can account for cell and viral measurements commonly observed during the three typical stages of HIV-1 disease. The model provides a means for organizing these elements into a comprehensive quantitative understanding of disease progression. It also elaborates optimal routes of therapy accounting for differences in disease progression and response to treatment between patients based on individual-specific host and viral factors.

The model yields both LTNP and typical progressor outcomes. The differences seen between these patients, as predicted by the model, are dependent on both viral and host factors. Viral infectivity and production rates strongly determine the progression rate of disease; this is corroborated by studies of R5 and X4 viral strains, where known differences in virulence are correlated with progression. The recognition and clearance of virus and infected cells by the immune response also strongly influences disease progression. In the simulations, increasing viral tropism and decreasing host response factors strongly influence the rate of disease progression.

We also incorporate HAART in the model by reducing viral infection and production rates and by increasing the source of $CD4^+$ T cells during the treatment phase. Model simulations of HAART show a rapid return of both lymphocyte cell subclasses, with memory preceding the naive class. The simulations also show a biphasic decline of virus in both blood and LT, indicating the presence of more than one class of viral production with differential dynamics. These phenomena are well documented in patients undergoing HAART. Consistent with the findings of clinical studies, the model also predicts a rapid rebound of virus when treatment is stopped. Ideally, treatment would contain viral production and infectivity such that treatment interruptions would be possible. Our model predicts that variations in both host and viral factors play a significant role in the development of an optimal treatment strategy.

APPENDIX

Model of Lymphocyte Circulation

Equations for naive (N) and memory (M) cells with the $\mathcal{B}$ and $\mathcal{L}$ subscripts denoting populations in the blood and lymphatic tissues (LT), respectively, are as follows:

$$N_{\mathcal{B}}'(t) = \beta e_{N\mathcal{L}} N_{\mathcal{L}}(t) - e_{N\mathcal{B}} N_{\mathcal{B}}(t) \quad (1)$$

$$M_{\mathcal{B}}'(t) = \beta e_{M\mathcal{L}} M_{\mathcal{L}}(t) - e_{M\mathcal{B}} M_{\mathcal{B}}(t) \quad (2)$$

$$N_{\mathcal{L}}'(t) = S_N(t) + \alpha e_{N\mathcal{B}} N_{\mathcal{B}}(t) - e_{N\mathcal{L}} N_{\mathcal{L}}(t) - \mu_N N_{\mathcal{L}}(t) \quad (3)$$

$$M_{\mathcal{L}}'(t) = \lambda \mu_N N_{\mathcal{L}}(t) + S_M(t) + \alpha e_{M\mathcal{B}} M_{\mathcal{B}}(t) - e_{M\mathcal{L}} M_{\mathcal{L}}(t) - \mu_M M_{\mathcal{L}}(t) \quad (4)$$

The first equation describes the rate of change of the uninfected naive cells in the blood, $N_{\mathcal{B}}(t)$. An influx of uninfected cells ($N_{\mathcal{L}}(t)$) circulating in from the LT at the rate $e_{N\mathcal{L}}$ is multiplied by β to scale* for exchange of units between compartments (from the LT to blood). Uninfected lymphocytes ($N_{\mathcal{B}}(t)$) emigrate from blood at rate $e_{N\mathcal{B}}$ to the LT. Equation 2 encompasses the same interactions for the uninfected memory cells in the blood. Exchange rates of memory cells to and from blood and the LT are $e_{M\mathcal{L}}$ (scaled by β) and $e_{M\mathcal{B}}$, respectively. Equation 3 represents the change in the number of naive cells in the LT ($N_{\mathcal{L}}(t)$) per day. Naive cells ($N_{\mathcal{B}}(t)$) arrive from the blood compartment at rate $e_{N\mathcal{B}}$ with scaling factor α and are lost to circulation (at rate $e_{N\mathcal{L}}$) or to natural death (μ_N). Similarly, memory cells die naturally (at rate μ_M), efflux from the LT at rate $e_{M\mathcal{L}}$, or influx from the blood ($e_{M\mathcal{B}}$).

We also allow for a small percentage of naive cells to directly differentiate from naive to memory during activation through division or differentiation (λ).

We include a source of naive cells in the LT ($S_N(t)$) similar to our assumptions of most dynamics occurring in the LT system as opposed

* To convert between the representation of cells and virus in blood, measured in cubic millimeters and milliliters, respectively, and that of LT measured in total cell/virus numbers, we use scaling factors (α and β) in the equations when describing exchange between the two compartments. Because there is 5 L of blood in the average human adult, when describing movement of $CD4^+$ T cells from blood to LT, we scale the terms by 5 L, or 5×10^6 μL. Describing circulation in the opposite direction, we scale by the inverse, or 2×10^{-7} μL of blood for $CD4^+$ T-cells and 4×10^{-4} mL for virus.

to the blood. It is believed that recent thymic emigrants of $CD4^+$ T cells are significantly lower in adults compared with children (27,28). To account for the influence of a slowly decaying source during aging, we include a decreasing input over our 10-year model time frame. The number of thymocytes entering blood is high during the first year of life and then decreases because of thymic involution at a rate of 5% per year between the ages of 25 and 40 years and at a rate of 0.1% thereafter (16,88). Thus, we assume that the source of naive cells decreases approximately 3% per year in an uninfected adult. Other ongoing work in our laboratory explores age-dependent decline in the lymphocyte population (89). This relation is represented by:

$$S_N(t) = \mu_N * N_{\mathcal{L}}(0) * 0.97^{\frac{t}{365}} \quad (5)$$

Similarly, the rate of change in memory cells in the LT is enhanced by a source ($S_M(t)$) as a result of proliferation and direct differentiation from the naive state. To maintain homeostasis of total $CD4^+$ T cells in both LT and blood, we estimate a memory cell population that remains inversely proportional to the number of naive cells. Instead of a mechanistic term for non-antigen-specific proliferation, we model the rate of change in source cells of memory class as a combination of proliferation and nonspecific antigen stimulation. This depends on the size of the naive cell class, thus reflecting a carrying capacity–dependent growth. Our model accounts for this mechanism with the following relation, where R and K_1 are constants (6.5×10^{19} and 1×10^{11}, respectively):

$$S_M(t) = \frac{R}{N_{\mathcal{L}}(t) + K_1} \quad (6)$$

Parameter Estimation for the Healthy Model

To fully derive the model systems (Equations 1–4), values for the parameters must be estimated. Often, parameter values can be obtained from literature; however, discrepancies in estimates from different sources result in a range of possible values. In this case, or when data are not available, we employ uncertainty and sensitivity analyses to study the effect of each parameter and explore the sensitivity of our model to their variations (49).

Values for blood $CD4^+$ T lymphocytes are typically measured in cells/mm^3 of blood and in total cell numbers for the lymphatic system. To estimate the number of $CD4^+$ lymphocytes in the blood, we begin with the value of 2×10^{11} to 1×10^{12} total lymphocytes in the body (4,16). Approximately 2% of these cells are present in the blood at any given time (41), totaling approximately 5×10^9 blood lymphocytes. Dividing this value by a blood volume of 5 L (for the average 70-kg adult human) yields 1000 cells/mm^3, the initial condition for total $CD4^+$ T cells ($N_{\mathcal{B}}(0) + M_{\mathcal{B}}(0)$). The ratio of naive to memory $CD4^+$ T cells is approximately 45% to 55% in an individual by the age of 20 years, respectively, in both blood and LT (16,90–92).

The input of cells to the naive and memory classes described previously is balanced by their respective lifespans. Some data indicate that the lifespan of a naive cell is approximately 7 weeks (7), although other data indicate that $CD45RA^+$ $CD62L^+$ lymphocytes have a half-life of 4 to 12 months (41,54). This yields a range of naïve cell death between 0.002 and 0.02 per day. Memory cells have been shown to have a half-life ranging from 1 to 2 months (41,54) up to almost 4 months, giving a death rate of 0.006 to 0.02 per day. Generally, it is thought that memory cells die one to two times as fast as naive cells because of their enhanced potential for activation, and thereby death (6,93). Thus, we assume a death rate for memory cells that is 1.5 times that of their naive counterparts.

Circulation rates were estimated based on the average time of 24 hours that a lymphocyte spends traveling through the LT (94,95). Lymphocytes exchange through the blood 48 times per day; thus, only 2% of the entire lymphocyte pool is present at any time in the blood (1,4,41).

In Table 1, we summarize the values used in the circulation model, which serve as a baseline for development of the subsequent models.

Infected Model Equations

Nine nonlinear ordinary differential equations describe the dynamics of the schematic outlined in Figure 3: four equations for rates of change

TABLE 1. *Parameter values for lymphocyte circulation model*

Variable	Definition	Initial value (reference)	Units
$N_{\mathcal{B}}(0)$	Uninfected naive $CD4^+$ T cells (blood)	450 (16)	Cells/mm^3 of blood
$M_{\mathcal{B}}(0)$	Uninfected memory $CD4^+$ T cells (blood)	550 (16)	Cells/mm^3 of blood
$N_{\mathcal{L}}(0)$	Uninfected naive $CD4^+$ T cells (LT)	9×10^{10} (16)	Cells
$M_{\mathcal{L}}(0)$	Uninfected memory $CD4^+$ T cell (LT)	1.1×10^{11} (16)	Cells
Parameter	**Definition**	**Value (reference)**	**Units**
α	Scaling term (blood → LT)	5×10^6	mm^3 or μL of blood
β	Scaling term (LT → blood)	2×10^{-7}	mm^3 or μL of blood
$e_{N\mathcal{L}}$	Circulation of naive cells (LT to blood)	1.0 (94, 95)	Day
$e_{N\mathcal{B}}$	Circulation of naive cells (blood to LT)	40.0 (94, 95)	Day
$e_{M\mathcal{L}}$	Circulation of memory cells (LT to blood)	0.25 (94, 95)	Day
$e_{M\mathcal{B}}$	Circulation of memory cells (blood to LT)	10.0 (94)	Day
μ_N	Death rate of uninfected naive cells (LT)	0.002 (41, 54)	Day
μ_M	Death rate of uninfected memory cells (LT)	0.003 (41, 54)	Day
S_N	Source of naive cells into LT	See Equation 5 (16, 88)	Cells/day
S_M	Proliferation of memory cells (LT)	See Equation 6 (63)	Cells/day
λ	Direct differentiation from naive to memory cells	0.1 (estimated)	Scalar

LT, lymphatic tissues.

of uninfected cells in the blood and LT (naive and memory cells), one equation for the rate of change of virus in each compartment, and equations for rates of change of the three infected classes in the LT:

$$N_{\mathcal{B}}'(t) = \beta e_{N\mathcal{L}} N_{\mathcal{L}}(t) - e_{N\mathcal{B}} N_{\mathcal{B}}(t) \quad (7)$$

$$M_{\mathcal{B}}'(t) = \beta e_{M\mathcal{L}} M_{\mathcal{L}}(t) - e_{M\mathcal{B}} M_{\mathcal{B}}(t) \quad (8)$$

$$N_{\mathcal{L}}'(t) = S_N(t) + \alpha e_{N\mathcal{B}} N_{\mathcal{B}}(t) - e_{N\mathcal{L}} N_{\mathcal{L}}(t) - k_N V_{\mathcal{L}}(t) N_{\mathcal{L}}(t) - \mu_N N_{\mathcal{L}}(t) + m_A A(t) \quad (9)$$

$$M_{\mathcal{L}}'(t) = \lambda \mu_N N_{\mathcal{L}}(t) + S_M(t) + \frac{\rho M_{\mathcal{L}}(t) V_{\mathcal{L}}(t)}{V_{\mathcal{L}}(t) + K_2} + \alpha e_{M\mathcal{B}} M_{\mathcal{B}}(t) - e_{M\mathcal{L}} M_{\mathcal{L}}(t) - k_M V_{\mathcal{L}}(t) M_{\mathcal{L}}(t) - \mu_M M_{\mathcal{L}}(t) \quad (10)$$

$$L'(t) = s_P P(t) - s_L L(t) - \gamma_L (N_{\mathcal{L}}(t) + M_{\mathcal{L}}(t)) * L(t) - \mu_L L(t) \quad (11)$$

$$P'(t) = p_{avg} * (k_N V_{\mathcal{L}}(t) N_{\mathcal{L}}(t) + k_M V_{\mathcal{L}}(t) M_{\mathcal{L}}(t)) - \gamma_P (N_{\mathcal{L}}(t) + M_{\mathcal{L}}(t)) * P(t) - \mu_P P(t) + s_L L(t) - s_P P(t) \quad (12)$$

$$A'(t) = q_{avg} * (k_N V_{\mathcal{L}}(t) N_{\mathcal{L}}(t) + k_M V_{\mathcal{L}}(t) M_{\mathcal{L}}(t)) - \gamma_A (N_{\mathcal{L}}(t) + M_{\mathcal{L}}(t)) * A(t) - m_A A(t) \quad (13)$$

$$V_{\mathcal{L}}'(t) = N \mu_P P(t) - e_V V_{\mathcal{L}}(t) - \mu_V V_{\mathcal{L}}(t) \quad (14)$$

$$V_{\mathcal{B}}'(t) = \beta e_V V_{\mathcal{B}}(t) - \gamma_V (N_{\mathcal{B}}(t) + M_{\mathcal{B}}(t)) * V_{\mathcal{B}}(t) - \mu_V V_{\mathcal{B}}(t) \quad (15)$$

Equations 7 and 8 remain as Equations 1 and 2 in the lymphocyte circulation model, because inflow and outflow from the blood compartment are the same in the absence and presence of virus. Equations 9 and 10 are altered with the addition of two mass action terms at rates k_N and k_M that model infection of naive and memory cells, respectively. The naive class also includes the addition of cells from the abortively infected class that revert to uninfected cells at conversion rate of m_A. T-cell production is also slightly altered during the course of HIV-1 infection (96). It has been estimated that the source of new thymus-derived $CD4^+$ T cells can decline to anywhere between 10% and 60% of the original value in some individuals, whereas there has been almost no effect in others (1,28). Thus, it is unclear how much thymic function is impaired in adult HIV-1 infection as well as to what extent the disease may influence thymic involution (1). Other work questions the general notion of thymic activity in adults (97). Thus, we alter Equation 5 from the baseline lymphocyte circulation model to account for an approximately 25% decrease in the source rate of new naive cells during virtual infection. The growth of $CD4^+$ memory T-cells in the lymphocyte circulation model was adequate to maintain an average of 1000 cells/mm^3. However, as our model simulations show, long-term nonprogressors (LTNPs) are able to maintain the immune response to infection through enhanced growth of the $CD4^+$ memory class beyond normal levels as a result of HIV-1 antigen presentation. This clonal expansion is reflected in a source of memory cells that proliferates proportional to the amount of antigen or virus present in the LT. Thus, we reflect this enhanced growth as a result of HIV-1 antigen presentation in Equation 4 from our baseline model by adding a term for HIV-1 antigen-induced memory cell proliferation, where ρ and K_2 are constants (0.005 and 5×10^8, respectively).

Equations 11 through 13 describe the rate of change in infected classes in the LT: latently (L(t)), productively (P(t)), and abortively (A(t)) infected cells. Infection of naive or memory cells directly leads to productive or abortive infections in proportions p and q, respectively. Each class has a natural life span or death rate. Latently infected cells can be activated and become productively infected at rate s_L, or productively infected cells can deactivate at rate s_P. The distinction between proportions of naive and memory cells that become productively or abortively infected has not yet been determined experimentally. Therefore, we model the contribution of infection from each class as an average proportion (p_{avg} and q_{avg}) based on estimates from data (37,40). Apoptosis of abortively infected cells is modeled as in previous work (3). This loss is described by estimating the value of m_A to account for the proportion of abortively infected cells (A(t)) that revert back to uninfected naive cells after a short period. Thus, the number of cells undergoing apoptosis is $1 - p_{avg} - q_{avg}$.

Virus is present in both the LT ($V_{\mathcal{L}}(t)$) and blood ($V_{\mathcal{B}}(t)$) compartments. Virus in the LT grows proportional to the number of productively infected cells. Of these virus-producing cells, each produces, on average, *N* virions over its life span (98). The only source of virus in blood is derived from the LT. Entry occurs at rate e_V, scaled by β.

There is a representative immune response against infected cell classes. The immune response to infection occurs primarily through the activity of $CD8^+$ CTLs acting on infected cells. There is a mass action immune response term in the LT for the three classes of infected cells at rates γ_L, γ_P, and γ_A. Because infected classes are not present in the blood compartment in our model, we indirectly model immune activity in the blood with γ_V, accounting for general clearance of virions in the blood. The immune response term of the form $\gamma_i(M_j + N_j)$ is represented as a function of the immune cells present at any given time point. In accordance with certain theories that DNA in latently infected cells remains invisible to immune surveillance, we investigate removal of the immune response to latently infected cells. We find that this makes no qualitative difference in disease progression.

Parameter Estimation for the Infected Model

The values used for the infection parameters presented in the LTNP model are detailed in Table 2. Virus titer in blood is typically measured as RNA copies/mL, whereas the lymphatic system is measured in total viral numbers. We outline below how we estimated their values. Our model steady states are robust to small changes in these parameter values as our sensitivity analyses confirm (see below).

Because the model is initiated at inoculum, other than the small amount of virus introduced in the LT, the initial conditions reflect that the other infected classes begin at zero.

Lifespans of productively infected cells are orders of magnitude shorter than those of uninfected cells. It is estimated that productively infected cells live for only 1 to 2 days (37,90,99), producing an adequate number of virions to infect new cells and sustain infection for years. One or 2 days after infection, most of the abortively infected cells have circulated back to the blood, undergoing rapid homing to the lymph nodes, where approximately 50% undergo apoptosis (5,25). The remainder of abortively infected cells can revert to the uninfected memory class after a period of 5 days based on the half-life of viral DNA (25), becoming potential candidates for future infection. Latently infected cells harbor integrated provirus. Sources claim this viral reservoir has a half-life of anywhere from 6 to 44 months (67,76,77). Of all the model components in our system, free virus has the shortest half-life of approximately 6 hours (19).

Infection rates of naive (k_N) and memory (k_M) cells account for infection of each cell subset meeting virus within the LT. These rates have been estimated per day per virion. We estimate an infection rate for naive cells greater than that for memory cells based on the discussion in the previous section.

The proportion of infected cells of each type is a subject of debate, mainly because of differences in classification from one study to the next. Productively infected cells are easiest to characterize because they are actively producing virus. This proportion is approximately 5 to 10

TABLE 2. *Parameter values used in models with HIV-1 infection*

Variable	Definition	Initial value (reference)	Units
L(0)	Latently infected $CD4^+$ T cells (LT)	0	Cells
P(0)	Productively infected $CD4^+$ T cells (LT)	0	Cells
A(0)	Abortively infected $CD4^+$ T cells (LT)	0	Cells
$V_{\mathcal{B}}(0)$	Virus concentration in blood	0	Virions/μL of blood
$V_{\mathcal{L}}(0)$	Virus (total) in LT	10 (can vary)	Virions
Parameter	**Definition**	**Value (reference)**	**Units**
e_V	Circulation of virus (LT to blood)	0.5 (estimated)	Day
μ_L	Death rate of latently infected T cells	0.000525 (76, 77)	Day
μ_P	Activation-induced cell death	0.5 (90, 100)	Day
μ_V	Death rate of free virus	3.0 (52, 98)	Day
k_N	Infection rate of naive cells by virus	8.0×10^{-12} (estimated)	Day—virion
k_M	Infection rate of memory cells by virus	1.0×10^{-12} (estimated)	Day—virion
p_{avg}	Proportion of productively infected cells	0.0187	Scalar
q_{avg}	Proportion of abortively infected cells that survive	0.675 (25)	Scalar
m_A	Reversion rate of abortively infected to naive cells	0.2 (36)	Day
s_L	Rate latently infected cells activate	0.03 (estimated)	Day
s_P	Rate productively infected cells deactivate	0.01 (estimated)	Day
N	Average virions produced by productively infected cells	500 (36)	Virions/cell
γ_v	Clearance rate of free virus (blood)	0.95 (estimated)	Day—cell
γ_L	Clearance rate of latently infected cells (LT)	2.0×10^{-13} (estimated)	Day—cell
γ_P	Clearance rate of productively infected cells (LT)	2.0×10^{-13} (estimated)	Day—cell
γ_A	Clearance rate of abortively infected cells (LT)	8.0×10^{-14} (estimated)	Day—cell

LT, lymphatic tissues.

cells per million or 10^5 per gram of lymphoid tissue (~1 in 100,000 cells) (16). The number of latently infected cells is similarly small, ranging from about 0.1% to 1% of the total number of infected cells or approximately 5 to 10 latently infected cells per million (40). Latently infected cells do not result from direct infection but from deactivation of productively infected cells (31,36). Abortively infected cells, resting cells that have come in contact with virus, exist at a ratio of about 7500 per million. Approximately 30% to 50% have been observed to undergo apoptosis (25).

A single productively infected cell can produce anywhere from 10^2 to 10^3 virions (25,50,51). As a starting estimate, we use a baseline value of viral production as 500 virions per day per cell and explore the full variation of this parameter within the text.

Because the CD4/CD8 ratio is observed to switch early in infection from 2:1 to 1:2 (17), our model indirectly accounts for this in our representation of the immune response. We model the $CD8^+$ T-cell response as proportional to the number of $CD4^+$ T cells present at any given point in disease progression.

Acknowledgments: This work was supported by National Institutes of Health grant HL62119–01. The authors thank Janis Wigginton for computing assistance and Ping Ye and the reviewers for helpful comments.

REFERENCES

1. Rosenberg Y, Janossy G. The importance of lymphocyte trafficking in regulating blood lymphocyte levels during HIV and SIV infections. *Semin Immunol* 1999;11:139–54.
2. Haase AT, Henry K, Zupancic M, et al. Quantitative image analysis of HIV-1 infection in lymphoid tissue. *Science* 1996;274: 985–9.
3. Kirschner D, Webb G, Cloyd M. Model of HIV-1 disease progression based on viral-induced lymph node homing and homing-induced apoptosis of $CD4^+$ lymphocytes. *J Aquir Immune Defic Syndr* 2000;24:352–62.
4. Rosenberg YJ, Anderson AO, Pabst R. HIV-induced decline in blood CD4/CD8 ratios: viral killing or altered lymphocyte trafficking? *Immunol Today* 1998;19:10–6.
5. Wang L, Robb CW, Cloyd MW. HIV induces homing of resting T lymphocytes to lymph nodes. *Virology* 1997;228:141–52.
6. Connors M, Kovacs JA, Krevat S, et al. HIV infection induces changes in CD4+ T-cell phenotype and depletions within the CD4+ T-cell repertoire that are not immediately restored by antiviral or immune-based therapies. *Nat Med* 1997;3:533–40.
7. Swain SL, Croft M, Dubey C, et al. From naive to memory T cells. *Immunol Rev* 1996;150:143–67.
8. Wack A, Cossarizza A, Heltai S, et al. Age-related modifications of the human alpha-beta T cell repertoire due to different clonal expansions in the CD4+ and CD8+ subsets. *Int Immunol* 1998; 10:1281–8.
9. Mackay CR, von Andrian UH. Memory T cells—local heroes in the struggle for immunity. *Science* 2001;291:2323–4.
10. Westermann J, Pabst R. Lymphocyte subsets in the blood: a diagnostic window on the lymphoid system? *Immunol Today* 1990:406–10.
11. Erkeller-Yuksel FM, Deneys V, Yuksel B, et al. Age-related changes in human blood lymphocyte subpopulations. *J Pediatr* 1992;120:216–22.
12. Hannet I, Erkeller-Yuksel F, Lydyard P, et al. Developmental and maturational changes in human blood lymphocyte subpopulations. *Immunol Today* 1992;13:215–8.
13. Hulstaert F, Hannet I, Deneys V, et al. Age-related changes in human blood lymphocyte subpopulations. *Clin Immunol Immunopathol* 1994;70:152–8.

14. Wiener D, Shah S, Malone J, et al. Multiparametric analysis of peripheral blood in the normal pediatric population by flow cytometry. *J Clin Lab Anal* 1990;4:175–9.
15. Yanase Y, Tango T, Okumura K, et al. Lymphocyte subsets identified by monoclonal antibodies in healthy children. *Pediatr Res* 1986;20:1147–51.
16. Haase A. Population biology of HIV-1 infection: viral and CD4+T cell demographics and dynamics in lymphatic tissues. *Annu Rev Immunol* 1999;17:625–56.
17. Margolick JB, Donnenberg AD. T-cell homeostasis in HIV-1 infection. *Semin Immunol* 1997;9:381–8.
18. Pantaleo G, Demarest JF, Schacker T, et al. The qualitative nature of the primary immune response to HIV infection is a prognosticator of disease progression independent of the initial level of plasma viremia. *Proc Natl Acad Sci USA* 1997;94:254–8.
19. Ho DD. Viral counts count in HIV infection. *Science* 1996;272: 1124–5.
20. Altfeld M, Rosenberg ES. The role of CD4+ T helper cells in the cytotoxic T lymphocyte response to HIV-1. *Curr Opin Immunol* 2000;12:375–80.
21. Comar M, Simonelli C, Zanussi S, et al. Dynamics of HIV-1 mRNA expression in patients with long-term nonprogressive HIV-1 infection. *J Clin Invest* 1997;100:893–903.
22. Pollard RB. Analogy of human immunodeficiency virus to hepatitis C virus: the human immunodeficiency model. *Am J Med* 1999;107(Suppl):S41–4.
23. Berkowitz RD, Alexander S, Bare C, et al. CCR5- and CXCR4-utilizing strains of human immunodeficiency virus type 1 exhibit differential tropism and pathogenesis in vivo. *J Virol* 1998;72: 10108–17.
24. Riley JL, Levine BL, Craighead N, et al. Naive and memory CD4 T cells differ in their susceptibilities to human immunodeficiency virus type 1 infection following CD28 costimulation: implications for transmission and pathogenesis. *J Virol* 1998;72: 8273–80.
25. Wang L, Chen JJ, Gelman BB, et al. A novel mechanism of CD4 lymphocyte depletion involves effects of HIV on resting lymphocytes: induction of lymph node homing and apoptosis upon secondary signaling through homing receptors. *J Immunol* 1999;162: 268–76.
26. Grossman Z, Paul WE. The impact of HIV on naive T-cell homeostasis. *Nat Am* 2000;6:976–7.
27. Zhang L, Lewin S, Markowitz M. Measuring recent thymic emigrants in blood of normal and HIV-1-infected individuals before and after effective therapy. *J Exp Med* 1999;190:725–32.
28. Douek DC, McFarland RD, Keiser PH, et al. Changes in thymic function with age and during the treatment of HIV infection. *Nature* 1998;396:690–5.
29. Hellerstein M, McCune J. T cell turnover in HIV-1 disease. *Immunity* 1997;7:583–9.
30. Hengel RL, Jones BM, Kennedy MS, et al. Markers of lymphocyte homing distinguish CD4 T cell subsets that turn over in response to HIV-1 infection in humans. *J Immunol* 1999;163: 3539–48.
31. Cloyd M, Chen J, Wang L. How does HIV cause AIDS? The homing theory. *Mol Med Today* 2000;6:108–11.
32. Gougeon M-L, Lecoeur H, Dulioust A, et al. Programmed cell death in peripheral lymphocytes from HIV-infected persons. *J Immunol* 1996;156:3509–20.
33. Muro-Cacho CA, Pantaleo G, Fauci AS. Analysis of apoptosis in lymph nodes of HIV-infected persons. Intensity of apoptosis correlates with the general state of activation of the lymphoid tissue and not with stage of disease or viral burden. *J Immunol* 1995; 154:5555–66.
34. Finkel TH, Tudor-Williams G. Apoptosis occurs predominantly in bystander cells and not in productively infected cells of HIV- and SIV-infected lymph nodes. *Nat Med* 1995;1:129–35.
35. Carbonari M, Pesce A, Cibati M. Death of bystander cells by a novel pathway involving early mitochondrial damage in HIV-related lymphadenopathy. *Blood* 1997;90:209–16.
36. Chen JJ, Cloyd MW. The potential importance of HIV-induction of lymphocyte homing to lymph nodes. *Int Immunol* 1999;11: 1591–4.
37. Ho DD. Dynamics of HIV-1 replication in vivo. *J Clin Invest* 1997;99:2565–7.
38. Michie CA, McLean A, Alcock C, et al. Lifespan of human lymphocyte subsets defined by CD45 isoforms. *Nature* 1992;360: 264–5.
39. Chun T-W, Stuyver L, Mizell SB, et al. Presence of an inducible HIV-1 latent reservoir during highly active antiretroviral therapy. *Proc Natl Acad Sci USA* 1997;94:13193–7.
40. Chun T-W, Carruth L, Finzi D, et al. Quantification of latent tissue reservoirs and total body viral load in HIV-1 infection. *Nature* 1997;387:183–8.
41. Richman DD. Normal physiology and HIV pathophysiology of human T-cell dynamics. *J Clin Invest* 2000;105:565–6.
42. Schrager LK, Fauci AS. Trapped but still dangerous. *Nature* 1995;377:680–1.
43. Li XD. Gradual shutdown of virus production resulting in latency is the norm during the chronic phase of human immunodeficiency virus replication and differential rates and mechanisms of shutdown are determined by viral sequences. *Virology* 1996;225:196–212.
44. Kaufmann G, Zaunders J, Murray J. Relative significance of different pathways of immune reconstitution in HIV type 1 infection as estimated by mathematical modelling. *AIDS Res Hum Retroviruses* 2001;17:147–59.
45. Pantaleo G, Menzo S, Vaccarezza M, et al. Studies in subjects with long-term nonprogressive human immunodeficiency virus infection. *New Engl J Med* 1995;332:209–16.
46. Greenough TC, Brettler DB, Kirchhoff F, et al. Long-term nonprogressive infection with human immunodeficiency virus type 1 in a hemophilia cohort. *J Infect Dis* 1999;180:1790–802.
47. Fauci AS, Pantaleo G, Stanley S, et al. Immunopathogenic mechanisms of HIV infection. *Ann Intern Med* 1996;124:654–63.
48. Miedema F, Tersmette M, van Lier RA. AIDS pathogenesis: a dynamic interaction between HIV and the immune system. *Immunol Today* 1990;11:293–7.
49. Blower S, Dowlatabadi H. Sensitivity and uncertainty analysis of complex models of disease transmission: an HIV model, as an example. *Int Stat Rev* 1994;62:229–43.
50. Tsai WP, Conley SR, Kung HF, et al. Preliminary in vitro growth cycle and transmission studies of HIV-1 in an autologous primary cell assay of blood-derived macrophages and peripheral blood mononuclear cells. *Virology* 1996;226:205–16.
51. Levy JA, Ramachandran B, Barker E. Plasma viral load, CD4+ cell counts, and HIV-1 production by cells. *Science* 1996;271: 670–1.
52. Stafford MA, Corey L, Cao Y, et al. Modeling plasma virus concentration during primary HIV infection. *J Theor Biol* 2000; 203:285–301.
53. Doms R, Peiper S. Unwelcomed guests with master keys: how HIV uses chemokine receptors for cellular entry. *Virology* 1997; 235:179–90.
54. Berger EA, Moss B, Pastan I. Reconsidering targeted toxins to eliminate HIV infection: you gotta have HAART. *Proc Natl Acad Sci USA* 1998;95:11511–3.
55. Miedema F, Meyaard L, Koot M, et al. Changing virus-host interactions in the course of HIV-1 infection. *Immunol Rev* 1994; 140:35–72.
56. Phillips AN, McLean AR, Loveday C, et al. In vivo replicative capacity in early and advanced infection. *AIDS* 1999;13:67–73.
57. Connor R, Sheridan K, Ceradini D, et al. Change in coreceptor use correlates with disease progression in HIV-1 infected individuals. *J Exp Med* 1997;185:621–8.
58. Collins K, Nabel G. Naturally attenuated HIV—lessons for AIDS vaccines and treatment. *N Engl J Med* 1999;340:1756–7.

59. Mehr R, Perelson AS. Blind T cell homeostasis and the CD4/CD8 ratio in the thymus and peripheral blood. *J Acquir Immune Defic Syndr Hum Retrovirol* 1997;14:387–98.
60. Caruso A, Licenziati S, Canaris AD, et al. Contribution of CD4+, CD8+CD28+, and CD8+CD28− T cells to CD3+ lymphocyte homeostasis during the natural course of HIV-1 infection. *J Clin Invest* 1998;101:137–44.
61. Saha K, Zhang J, Gupta A. Isolation of primary HIV-1 that target CD8+ T lymphocytes using CD8 as a receptor. *Nat Med* 2001; 7:65–72.
62. Saha K, Zhang J, Zerhouni B. Evidence of productively infected $CD8^+$ T cells in patients with AIDS: implications for HIV-1 pathogenesis. *J Acquir Immune Defic Syndr* 2001;26:199–207.
63. Roederer M, De Rosa SC, Watanabe N, et al. Dynamics of fine T-cell subsets during HIV disease and after thymic ablation by mediastinal irradiation. *Semin Immunol* 1997;9:389–96.
64. Sabin CA, Devereux H, Phillips AN, et al. Course of viral load throughout HIV-1 infection. *J Acquir Immune Defic Syndr* 2000; 23:172–7.
65. Pantaleo G, Graziosi C, Fauci AS. Mechanisms of disease: the immunopathogenesis of human immunodeficiency virus infection. *N Engl J Med* 1993;328:327–35.
66. Chun T-W, Justement JS, Moir S, et al. Suppression of HIV replication in the resting CD4+ T cell reservoir by autologous CD8+ T cells: implications for the development of therapeutic strategies. *Proc Natl Acad Sci USA* 2001;98:253–8.
67. Pierson T, McArthur J, Siliciano RF. Reservoirs for HIV-1: mechanisms for viral persistence in the presence of antiviral immune responses and antiretroviral therapy. *Annu Rev Immunol* 2000;18:665–708.
68. Battegay M. Human immunodeficiency virus mutation and changes in CD4 T-cell levels during antiretroviral therapy. *Eur J Clin Microbiol Infect Dis* 1998;17:301–3.
69. Pakker NG, Notermans DW, De Boer RJ, et al. Biphasic kinetics of peripheral blood T cells after triple combination therapy in HIV-1 infection: a composite of redistribution and proliferation. *Nat Med* 1998;4:208–14.
70. Kelleher AD, Carr A, Zaunders J, et al. Alterations in the immune response of human immunodeficiency virus (HIV)-infected subjects treated with an HIV-specific protease inhibitor, ritonavir. *J Infect Dis* 1996;173:321–9.
71. Autran B, Carcelain G, Li T, et al. Positive effects of combined antiretroviral therapy on CD4+ T cell homeostasis and function in advanced HIV disease. *Science* 1997;277:112–6.
72. Zhang Z-Q, Notermans DW, Sedgewick G, et al. Kinetics of CD4+ T cell repopulation of lymphoid tissues after treatment of HIV-1 infection. *Proc Natl Acad Sci USA* 1998;95:1154–9.
73. Franco JM, Leon-Leal JA, Leal M, et al. CD4+ and CD8+ T lymphocyte regeneration after anti-retroviral therapy in HIV-1-infected children and adult patients. *Clin Exp Immunol* 2000;119: 493–8.
74. Ferguson NM, deWolf F, Ghani AC, et al. Antigen-driven CD4+ T cell and HIV-1 dynamics: residual viral replication under highly active antiretroviral therapy. *Proc Natl Acad Sci USA* 1999;96:15167–72.
75. Chun T-W, Davey RT, Jr, Engel D, et al. Re-emergence of HIV after stopping therapy. *Nature* 1999;401:874–5.
76. Saag MS, Kilby JM. HIV-1 and HAART: a time to cure, a time to kill. *Nat Med* 1999;5:609–11.
77. Chun T-W, Fauci AS. Latent reservoirs of HIV: obstacles to the eradication of virus. *Proc Natl Acad Sci USA* 1999;96:10958–61.
78. Kuster H, Opravil M, Ott P, et al. Treatment-induced decline of human immunodeficiency virus-1 p24 and HIV-1 RNA in lymphoid tissue of patients with early human immunodeficiency virus-1 infection. *Am J Pathol* 2000;156:1973–86.
79. Kilby JM, Goepfert PA, Miller AP, et al. Recurrence of the acute HIV syndrome after interruption of antiretroviral therapy in a patient with chronic HIV infection: a case report. *Ann Intern Med* 2000;133:435–8.
80. Ho DD, Zhang L. HIV-1 rebound after anti-retroviral therapy. *Nat Med* 2000;6:736–7.
81. Zhang L, Ramratnam B, Tenner-Racz K, et al. Quantifying residual HIV-1 replication in patients receiving combination antiretroviral therapy. *N Engl J Med* 1999;340:1605–13.
82. Furtado MR, Callaway DS, Phair JP, et al. Persistence of HIV-1 transcription in peripheral blood mononuclear cells in patients receiving potent antiretroviral therapy. *N Engl J Med* 1999;340: 1614–22.
83. Garcia F, Vidal C, Plana M, et al. Residual low-level viral replication could explain discrepancies between viral load and CD4+ cell response in human immunodeficiency virus-infected patients receiving antiretroviral therapy. *Clin Infect Dis* 2000;30:392–4.
84. Davey RT, Bhat N, Yoder C, et al. HIV-1 and T cell dynamics after interruption of highly active antiretroviral therapy (HAART) in patients with a history of sustained viral suppression. *Proc Natl Acad Sci USA* 1999;96:15109–14.
85. Notermans DW, Pakker NG, Hamann D, et al. Immune reconstitution after 2 years of successful potent antiretroviral therapy in previously untreated human immunodeficiency virus type 1-infected adults. *J Infect Dis* 1999;180:1050–6.
86. Kirschner D, Webb GF. A model for treatment strategy in the chemotherapy of AIDS. *Bull Math Biol* 1996;58:376–90.
87. Ortiz GM, Nixon DF, Trkola A, et al. HIV-1-specific immune responses in subjects who temporarily contain virus replication after discontinuation of highly active antiretroviral therapy. *J Clin Invest* 1999;104:R13–8.
88. Steinmann GG, Klaus B, Muller-Hermelink HK. The involution of the ageing human thymic epithelium is independent of puberty. *Scand J Immunol* 1985;22:563–75.
89. Ye P, Kirschner D. Re-evaluation of T cell receptor excision circles as a measure of human recent thymic emigrants. *J Immunol* 2002, in press.
90. Cavert W, Notermans DW, Staskus K, et al. Kinetics of response in lymphoid tissues to antiretroviral therapy of HIV-1 infection. *Science* 1997;276:960–4.
91. Hayward AR: Lymphoid cell development. *Immunol Ser* 1989; 43:145–62.
92. Essunger P, Perelson AS. Modeling HIV infection of CD4+ T-cell subpopulations. *J Theor Biol* 1994;170:367–91.
93. Clark DR, De Boer RJ, Wolthers KC, et al. T-cell dynamics in HIV-1 infection. *Adv Immunol* 1999;73:301–27.
94. Sprent J, Basten A. Circulating T and B lymphocytes of the mouse, II. Lifespan. *Cell Immunol* 1973;7:40–59.
95. Sprent J. Circulating T and B lymphocytes of the mouse, I. Migratory properties. *Cell Immunol* 1973;7:10–39.
96. McCune J. The dynamics of CD4+ T-cell depletion in HIV disease. *Nature* 2001;410:974–9.
97. McCune JM, Loftus R, Schmidt DK, et al. High prevalence of thymic tissue in adults with human immunodeficiency virus-1 infection. *J Clin Invest* 1998;101:2301–8.
98. Perelson AS, Kirschner DE, DeBoer R. Dynamics of HIV infection of CD4+ T cells. *Math Biosci* 1993;114:81–125.
99. Perelson AS, Neumann AU, Markowitz M, et al. HIV-1 dynamics in vivo: virion clearance rate, infected cell life-span, and viral generation time. *Science* 1996;271:1582–6.